Sixth International Symposium on Turbulence and Shear Flow Phenomena
Seoul, Korea, 22-24 June 2009

EXPERIMENTAL INVESTIGATION OF TURBULENT WAKE BEHIND A SPHERE AT A SUBCRITICAL REYNOLDS NUMBER

Young Il Jang
Department of Aerospace and Mechanical Engineering,
Korea Air Force Academy
P.O.Box 335-2, Cheongwon, Choongbuk, 363-849, Korea
yijang@airforce.mil.kr

Sang Joon Lee
Department of Mechanical Engineering,
Pohang University of Science and Technology
San 31, Hyoja, Namgu, Pohang, Kyungbuk, 790-784, Korea
sjlee@postech.ac.kr

ABSTRACT

The flow characteristics of near-wake and turbulent flow over a sphere at a subcritical flow regime were experimentally investigated. The qualitative and quantitative results obtained from smoke-wire visualization, PIV measurements and POD(proper orthogonal decomposition) modal analysis were used to get detailed flow information such as laminar to turbulent transition, vortex formation, vortex shedding, shear-layer instability, wavy structure of wake and coherent structures of the sphere wake. The detailed turbulent structure of sphere wake such as recirculating flow, shear layer instability, vortex roll-up, and small-scale turbulent eddies were clearly visualized. In the streamwise center plane, mean velocity field had two large-scale recirculation vortices, of which the recirculation length was about x/d=1.05. In the cross-sectional planes, the instantaneous vorticity fields revealed an unsteady wavy structure of the sphere wake. The regions of large values of turbulence statistics such as turbulent intensities and turbulent kinetic energy were closely related to the onset of shear layer instability in the near-wake behind the sphere model. That is, the location of the local maximum turbulence statistics both in the streamwise and cross-sectional planes corresponded to the onset location of shear layer instability observed in the visualized flow fields at x/d=1.0~1.2. The relative contribution of the POD mode 1, 2 and 3 in eigenvalues was 26, 11, and 8 %, respectively. The velocity fields for the POD mode 1 at the near-wake region of x/d=0.7-1.4 in the cross-sectional planes showed similar pattern with those of time-averaged mean velocity fields. In addition, the unique pattern of sweeping flow in the region from x/d=1.5 to x/d=2.0 showed the wavy structure of the sphere wake along the streamwise direction. This implies that the wavy pattern is the dominant coherent structure of the sphere wake. These experimental results on sphere near-wake would contribute to the fundamental understanding of the turbulent wake flow behind a sphere and provide useful data for validating numerical prediction at a subcritical flow regime.

BACKGROUND AND OBJECTIVES

A sphere is considered as the idealized model of three-dimensional axi-symmetric bluff bodies. To design low drag vehicles or to apply flow control schemes to a bluff body, an understanding of the physical nature of the flow around a sphere is essential. Although a spherical body is perfectly axi-symmetric, the vortical structure around it has been known to show diverse flow characteristics such as axi-symmetric flow, planar symmetric flow, and irregular rotation of separation points, unsteady flow, periodic vortex shedding, laminar wake, shear layer instability, turbulent wake, and turbulent separation, depending on the Reynolds number.

The present study is to visualize the instantaneous turbulent flow over a sphere at Re=11,000 and 5,300 using an improved smoke-wire method. And, the vortical structures of sphere wake in the streamwise plane at Re=11,000 are measured using a PIV technique to clarify recirculating vortices, recirculation length, and the spatial distributions of turbulence statistics. Moreover, the vortical structures in the cross-sectional planes are also studied using the same PIV technique to get the spatial distributions of in-plane velocities, vorticity, and turbulence statistics in the near-wake. Furthermore, the POD modal characteristics of coherent structure are to be analyzed by deriving eigenvalues and spatial modes by the snapshots method in the cross-sectional planes. Through these systematic experiments, we hope to understand not only the vortex formation, vortex shedding, shear-layer instability but also wavy structure, swirling characteristics and coherent structures in the near-wake over a sphere at a subcritical flow regime.

PIV METHOD

As shown in Fig. 1(a), the streamwise (x-y) center plane was illuminated simultaneously both from the upper and lower sides of the test section with thin laser light using a beam splitter, mirrors, and cylindrical lenses. Therefore, the whole field around the sphere did not have any shaded region. The thickness of the laser light sheet was about 3 mm. The PIV system consisted of a two-head Nd:YAG laser (New Wave) of 125 mJ, a CCD camera (Kodak) of 2K×2K pixels resolution, and a delay generator. A 35 mm micro lens was fitted in front of the CCD camera. The laser and the high-resolution CCD camera were synchronized by the delay generator. The field of view was 26×26 cm^2, covering the range from x=-0.7d to x=+2.8d along the streamwise direction.

The cross-sectional (y-z) plane was illuminated from the bottom side of the test section as shown in Fig. 1(b). For this experiment, the CCD camera was fitted with a 105 mm micro lens and was inserted into a water-resistant case for installation inside the test section. The distance between the sphere model and the CCD camera was 20 times the sphere diameter in order to minimize the disturbance caused by the presence of the CCD camera in downstream. The field of view in the cross-sectional plane was 15×15 cm^2, covering the area ranging from z=-1.0d to z=+1.0d. The particle images of the flow were acquired at 17 cross-sections from x/d=0.5 to x/d=2.2 by scanning the laser light sheet using a precise traverse system and corresponding focus of the CCD camera.

Spherical silver particles having an average diameter of 10μm were used as tracer particles. Five hundred pairs of PIV particle images were captured at a 4 Hz sampling rate for each experimental condition. The two-frame cross-correlation method was employed to extract velocity vector fields from the particle images. The interrogation window was 64×64 pixels with 50% overlapping.

VALIDATION OF MODEL INSTALLATION

To support the sphere model in the test section, the two piano wires of 0.17 mm in diameter were inserted through the sphere center in 'X'-shape, facing upwards perpendicularly. The ends of the four wires were fastened firmly to the frame of the water channel with precise turnbuckles. The structural vibration of the sphere model installed in a wind tunnel test section with fine wires was evaluated by using a non-contact laser vibrometer(Fig. 2(a)). The fastest vibrational velocity and the one period are -1.6 mm/s and 3.9s, respectively, in z-direction. The maximum vibrational displacement would be less than 6 nm. The dominant frequency appears at f_v=256 kHz and there is no dominant vibration in low frequency range. It turns out that the effect of model vibration to the wake flow is negligible, comparing the order of magnitude in model vibrational frequency and displacement with that of the wake flow.

FORMULATION OF POD

Since turbulent flows involve complicated interaction of many degrees of freedom over broad ranges of spatial and temporal scales, the small-scale turbulence is embedded in the large-scale and vice versa. Coherent structures are organized features which repeatedly appear and undergo a characteristic temporal cycle (Berkooz et al., 1993). POD offers a rational method to extract coherent structure. POD is a modal description for coherent structures which are dominant modes containing high turbulent kinetic energy. It enables us to reconstruct each dominant instantaneous velocity field. Using POD modal analysis, flow characteristics of the near-wake and turbulent flow over a sphere can be revealed in different point of view, which are difficult to see in the time-averaged analysis.

The mathematical formulation of POD has been well established by several researchers (Holmes et al., 1996; Berkooz et al., 1993; Sirovich, 1987). In Reynolds decomposition, an instantaneous velocity can be decomposed into mean velocity and fluctuating velocity component. In POD, the fluctuating velocity component can be expressed as the sum of temporal mode coefficients a_n uncorrelated with time, multiplied by normalized base functions ϕ_n which are spatially orthogonal.

$$u(\vec{x},t) = U(\vec{x}) + \sum_{n=1}^{N} a_n(t)\phi_n(\vec{x}) \tag{1}$$

SMOKE-WIRE VISUALIZATION RESULTS

Figure 3 shows the instantaneous flow visualizations around a sphere model at Re=11,000, which were obtained with smoke-wire positioned behind the sphere model. The recirculating region filled with smoke filaments convected upstream behind the sphere is observed. The laminar flow separation occurs near the equator of the sphere model and the laminar shear layer is axisymmetrically stable until x/d =1.0~1.2. At this point, the shear layer becomes unstable due to the Kelvin-Helmholtz instability. Thereafter, the laminar shear layer turns into turbulent flow. The vortex-ring shaped protrusions are observed. The detailed turbulent structure of sphere wake such as recirculating flow, shear layer instability, vortex roll-up, and small-scale turbulent eddies were clearly visualized.

PIV RESULTS

Five hundred instantaneous velocity fields were obtained for each experimental condition in PIV measurements. In order to obtain the dominant shedding frequency, we carried out the spectral analysis using the velocity signal V_x extracted at x/d=0.98, y/d=0.47 from the measured instantaneous velocity field data. The shedding frequency was 0.298 and the corresponding Strouhal number was St=0.175. The value of St number agrees well with the results of Suryanarayana and Prabhu(2000) and Sakamoto and Haniu(1990). Two large-scale recirculation vortices formed behind a sphere are nearly symmetrical with respect to the wake centerline (y=0). The length of the recirculation region extends to x/d=1.05.

Some of the temporal evolution of instantaneous vorticity field in the cross-sectional plane at x/d=1.5 is shown in Fig. 4. Active vortices seem to be concentrated at the center and are stretched outward. Vortical structures are similar to one another except in the stretched direction. The main direction of the active vortices belongs to a quarter irregularly of the wake region. Vortices with opposite rotation direction and different strengths are distributed in an irregular manner with lapse of time, and the maximum strength of vorticity also changes with time. The wavy flow structure of the sphere wake in the streamwise plane has been reported in several studies (Taneda 1978; Sakamoto and Haniu 1990; Leder and Geropp 1993). However, the waviness of the sphere wake in the cross-sectional planes has not been measured yet.

Figure 5 shows the spatial distribution of turbulence intensities. Figure 5(a) shows that the spatial distribution of has large values in tilted elliptic-shaped contours and that the local maximum value occurs at x/d=1.05. In the cross-sectional planes, the turbulence intensity has large values around the sphere periphery at x/d=0.8. With going downstream, the location of the local maximum value moves toward the wake center, and its magnitude becomes the maximum at x/d =1.2 as seen in Fig. 5(b). The contours show a concentric shape centered at the wake center (y=0, z =0). The regions of large turbulent statistical values seem to be closely related to the onset of shear layer instability in the near-wake behind the sphere model. The location of the local maximum turbulence intensities in Fig. 5 corresponds to the onset location of shear layer instability in Fig. 3.

POD ANALYSIS

The POD modal characteristics of the turbulent wake in the cross-sectional planes behind a sphere at Re=11,000 were analyzed with the POD eigenvalues and modal velocity vector fields. Figure 6(a) shows the convergence of the normalized eigenvalues. The accumulated sum of eigenvalues, normalized by the total sum of eigenvalues, reaches 0.99 at mode 201. The relative contribution of the POD mode 1, 2 and 3 in eigenvalues was 26, 11, and 8 %, respectively. Velocity vector fields of the POD mode 1 at x/d=0.7-1.4 showed similar pattern with those of time-averaged velocity fields. On the other hand, the sphere wake in the region from x/d=1.5 to x/d=2.0 showed the directional variation of flow pattern at sequential x/d locations. This implies that the wavy pattern was the dominant coherent structure of the sphere wake. From the POD mode 2, the conspicuous foci, saddle and node points appeared irregularly at each downstream locations. The unique distribution patterns including the large-scale circulatory vortex in the POD modes were not observed in instantaneous or time-averaged mean velocity fields.

REFERENCES

Achebach, E., 1972, “Experiments on the flow past spheres at very high Reynolds numbers”, *J. Fluid Mech*., Vol. 54, pp. 565-575.

Achebach, E., 1974, “Vortex shedding from spheres”, *J. Fluid Mech.*, Vol. 62, pp. 209-221.

Berkooz, G., Holmes, P., and Lumley, J.L., 1993, “The proper orthogonal decomposition in the analysis of turbulent flows”, *Annu. Rev. Fluid Mech.*, Vol. 25, pp. 539-575.

Constantinescu, G. S., and Squires, K. D., 2004, “Numerical investigations of flow over a sphere in the subcritical and supercritical regimes”, *Phys. Fluids*, Vol. 16, pp. 1449-1466.

Holmes, P., Lumley, J.L., and Berkooz, G., 1996, *Turbulence, coherent structures, dynamical systems and symmetry*, Cambridge university press.

Kim, H. J., and Durbin, P. A., 1988, “Observations of the frequencies in a sphere wake and of drag increase by acoustic excitation”, *Phys. Fluids*, Vol. 31, pp. 3260-3265.

Lee, S. J., and Lee, S. H., 1999, “Synchronized smoke-wire technique for flow visualization of turbulent flows”, *J. Flow Vis. & Image Proc*., Vol. 6, pp. 65-78.

Manhart, M., and Wengle, 1993, “A spatiotemporal decomposition of a fully inhomogeneous turbulent flow field”, *Theoret. Comput. Fluid Dynamics*, Vol. 5, pp. 223-242.

Perry, A. E., and Chong, M. S., 1987, “A description of eddying motions and flow patterns using critical-points concepts”, *Ann. Rev. Fluid Mech*., Vol. 19, pp. 125-155.

Sirovich, L., 1987, “Turbulence and the dynamics of coherent structures”, *Quart. Appl. Math.*, Vol. 45, pp. 561-590.

Suryanarayana, G. K., and Prabhu, A., 2000, “Effect of natural ventilation on the boundary layer separation and near-wake vortex shedding characteristics of a sphere”, *Exp. Fluids* Vol. 29, pp. 582-591.

Sakamoto, H., and Haniu, H., 1990, “A study on vortex shedding from spheres in a uniform flow”, *J. Fluids Eng*., Vol. 112, pp. 386-392.

Taneda, S., 1978, “Visual observations of the flow past a sphere at Reynolds numbers between 10^4 and 10^6”, *J. Fluid Mech.*, Vol. 85, pp. 187-192.

Leder, A., and Geropp, D., 1993, “The unsteady flow structure in the wake of the sphere”, *SPIE* Vol. 2052, pp. 119-126.

Werlé, H., 1980, *ONERA photograph* In: An album of fluid motion(assembled by Dyke V), pp. 32-35, Parabolic Press, CA.

Yi, S. J., Kim, J. W., Kim, H. D., and Kim, K. C., 2008, “Characteristics of bubble-driven flow by using time-resolved PIV and POD technique”, *J. Korean Soc. Visualization*, Vol. 6, pp. 41-46.

Yun, G., Kim, D., and Choi, H., 2006, “Vortical structures behind a sphere at subcritical Reynolds numbers”, *Phys. Fluids*, Vol. 18, p. 015102.

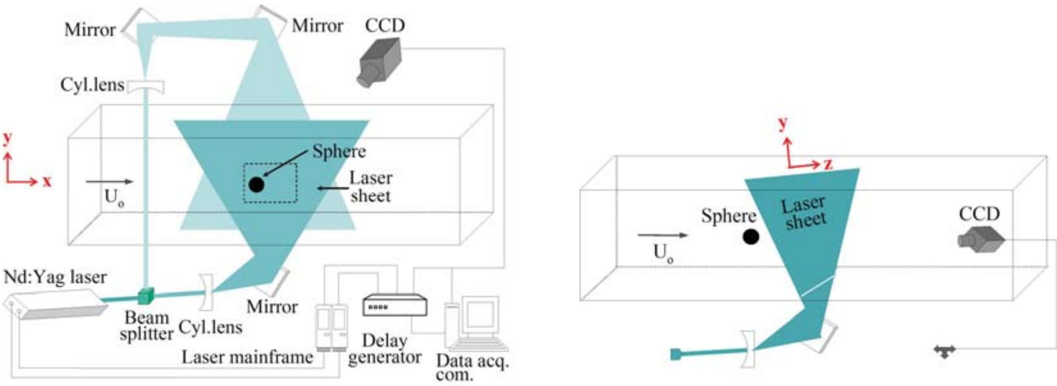

(a) Streamwise (*x*-*y*) plane (b) Cross-sectional (*y*-*z*) plane

Fig. 1 Schematic diagram of PIV measurement system

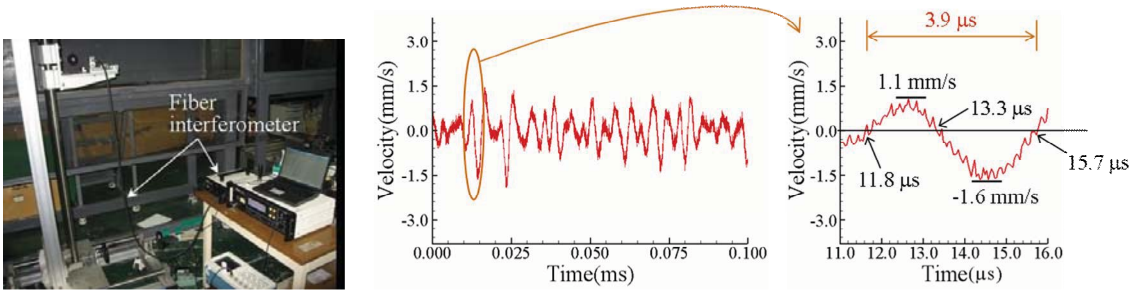

(a) Setup (b) Vibrational velocity with time

Fig. 2 Setup of laser Doppler vibrometer and its result in *z*-direction

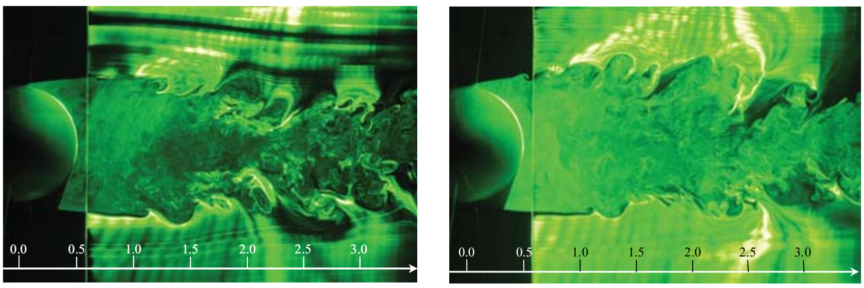

Fig. 3 Instantaneous visualization of flow around a sphere at Re=11,000

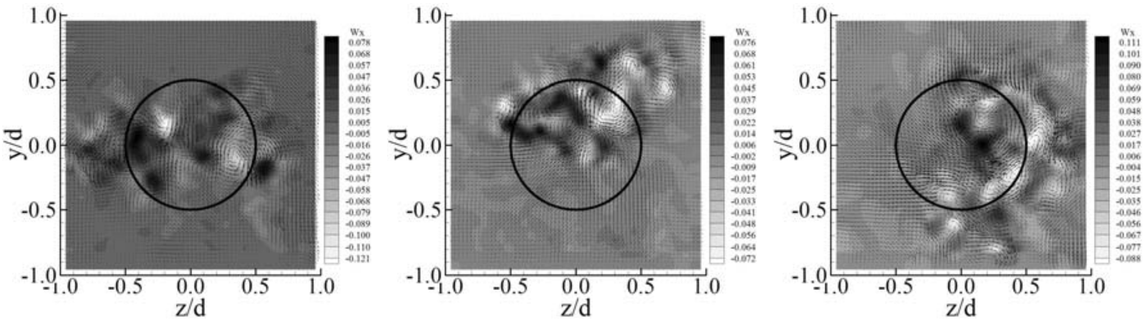

(a) t^*=0 (b) t^*=0.43 (c) t^*=0.87

Fig. 4 Instantaneous vorticity contours in the cross-sectional plane at x/d=1.5 at Re=11,000

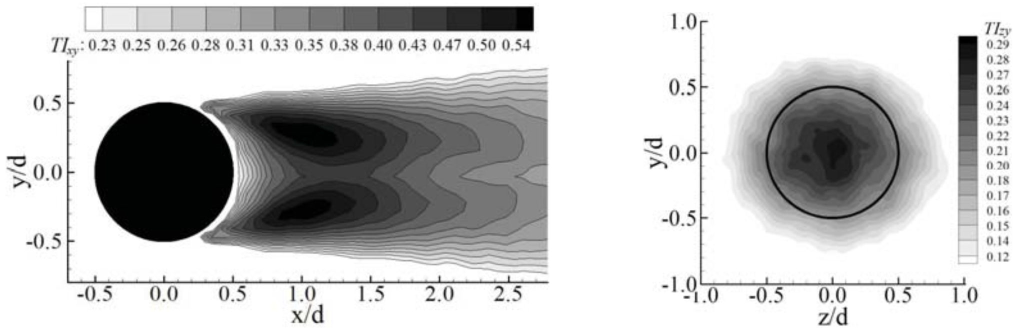

(a) $\left(\sqrt{\overline{V_x'^2}}+\sqrt{\overline{V_y'^2}}\right)/2U_o$ (%) (b) $\left(\sqrt{\overline{V_z'^2}}+\sqrt{\overline{V_y'^2}}\right)/2U_o$ (%) at x/d=1.2

Fig. 5 Turbulence intensity distributions in the streamwise and cross-sectional planes at Re=11,000

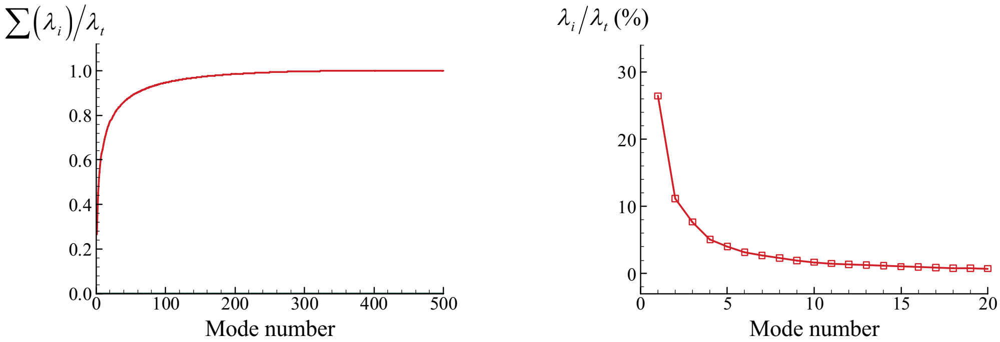

(a) Convergence of normalized eigenvalues (b) Relative contributions of fore 20 eigenvalues

Fig. 6 Convergence and relative contribution of eigenvalues in the cross-sectional planes at Re=11.000

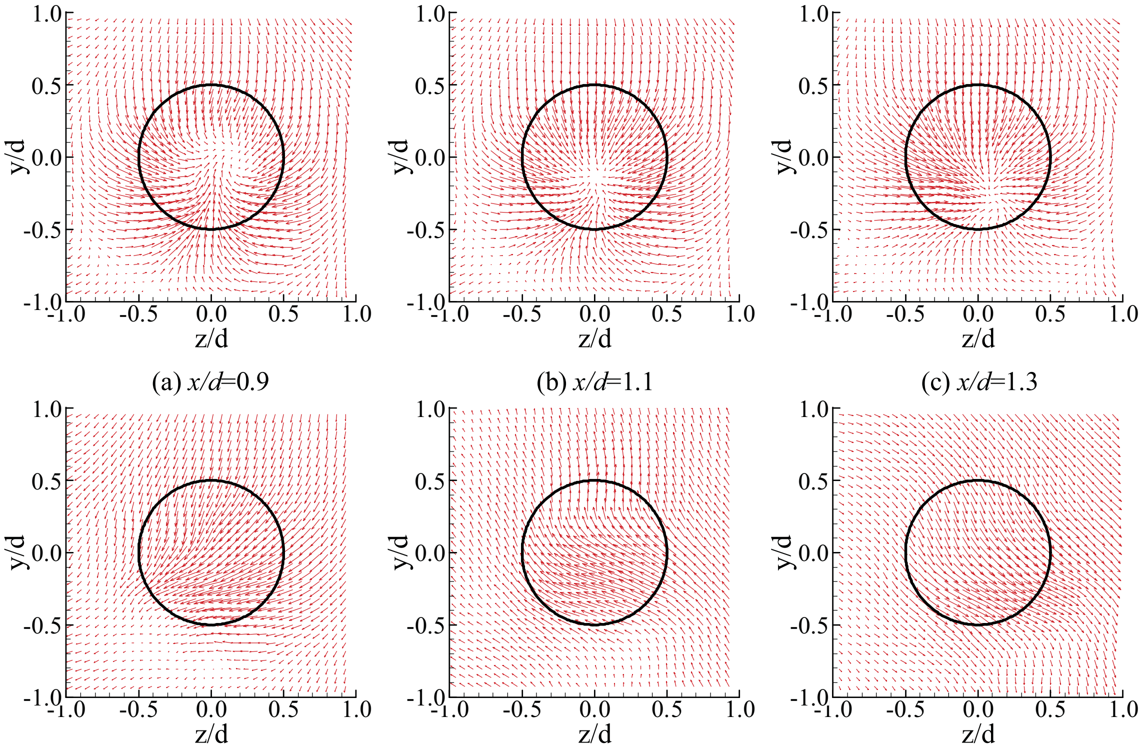

(a) x/d=0.9 (b) x/d=1.1 (c) x/d=1.3

(d) x/d=1.5 (e) x/d=1.7 (f) x/d=1.9

Fig. 7 Velocity vector fields of POD mode 1 in the cross-sectional planes at Re=11,000